GATA2-Mediated Transcriptional Activation of Notch3 Promotes Pancreatic Cancer Liver Metastasis

Heng Lin[1,2], Peng Hu[1,2], Hongyu Zhang[1], Yong Deng[1], Zhiqing Yang[1,]*, and Leida Zhang[1,]*

[1]Institute of Hepatobiliary Surgery, Southwest Hospital, Third Military Medical University (Army Medical University), Chongqing 400038, China, [2]These authors contributed equally to this work.
*Correspondence: yzq1977@outlook.com (ZY); raderlh@tmmu.edu.cn (LZ)
https://doi.org/10.14348/molcells.2022.2176
www.molcells.org

The liver is the predominant metastatic site for pancreatic cancer. However, the factors that determine the liver metastasis and the specific molecular mechanisms are still unclear. In this study, we used human pancreatic cancer cell line Hs766T to establish Hs766T-L3, a subline of Hs766T with stable liver metastatic ability. We performed RNA sequencing of Hs766T-L3 and its parental cell line Hs766T, and revealed huge differences in gene expression patterns and pathway activation between these two cell lines. We correlated the difference in pathway activation with the expression of the four core transcriptional factors including STAT1, NR2F2, GATA2, and SMAD4. Using the TCGA database, we examined the relative expression of these transcription factors (TFs) in pan-cancer and their relationship with the prognosis of the pancreatic cancer. Among these TFs, we considered GATA2 is closely involved in tumor metastasis and may serve as a potential metastatic driver. Further *in vitro* and *in vivo* experiments confirmed that GATA2-mediated transcriptional activation of Notch3 promotes the liver metastasis of Hs766T-L3, and knockdown of either GATA2 or Notch3 reduces the metastatic ability of Hs766T-L3. Therefore, we claim that GATA2 may serve as a metastatic driver of pancreatic cancer and a potential therapeutic target to treat liver metastasis of pancreatic cancer.

Keywords: GATA2, liver metastasis, Notch3, RNA sequencing

INTRODUCTION

Pancreatic cancer is an aggressive disease with the second leading cause of cancer mortality within a decade (Siegel et al., 2019). Early diagnosis of pancreatic cancer is still difficult, and most patients are diagnosed as advanced stage with poor prognosis (Li et al., 2004). Liver metastasis occurred in 70% of patients with pancreatic cancer, and the metastatic lesions may be colonized before surgery, which is one of the most common reasons for treatment failure (Ducreux et al., 2015). The median survival time of patients with liver metastases from pancreatic cancer is less than 6 months (Siegel et al., 2017). Once liver metastases occur, therapeutic resection is impossible. Further clarification of the specific mechanisms of liver metastasis will help to identify patients with greater risk of cancer progression and provide new strategies for the treatment of pancreatic cancer metastasis.

Traditional views regarded that metastasis is a result of a small number of cancer cells acquiring specific genetic changes that drive them to spread and colonize in distant organs (Fidler and Kripke, 1977; Poste and Fidler, 1980). Recently, increasing evidence showed that cancer metastasis may be directly driven by mutation and overexpression of a number of core genes, and the expression patterns of these genes are significant different in subpopulations of cancer cells with different metastatic ability (Ramaswamy et al., 2003; van 't Veer

et al., 2002). For example, a previous study reported that bone metastasis of breast cancer cells is mediated by a specific set of genes including CTGF, IL-11, CXCR-4, and MMP-1, these genes are overexpressed in the subpopulations of breast cancer cells with high metastatic activity, and mediate the specific bone metastasis and cancer-induced osteolysis (Kang et al., 2003; Liang et al., 2019). These studies provide a conceptual foundation and experimental methods for the subsequent establishment of cancer cell lines with high metastatic activity and identification of genes mediating metastasis.

Transcription factors (TFs) regulate the transcriptional activity of downstream target genes to be involved in multiple biological progresses of cancer progression including tumorigenesis, angiogenesis, and immune escape (Di Genua et al., 2020; Mohan et al., 2020). As the primary TFs in this study, STAT1, NR2F2, GATA2, and SMAD4 were shown to be associated with the tumorigenesis and cancer progression. Specifically, the roles of STAT1 in cancer progression are still controversial. Several studies have reported that STAT1-mediated transcriptional activation of target genes including estrogen receptor α (ERα), chemokine (C-X-C motif) ligand 1 (CXCL1), and C-myc stimulates proliferation, invasion of cancer cells as well as immune suppression (Hou et al., 2018; Liang et al., 2019; Liu et al., 2019b). Other studies have shown that STAT1 has been involved in the activation of antitumor immune responses and enhancement of drug sensitivity (Liu et al., 2019a; Ryan et al., 2020). NR2F2 is a nuclear receptor serving as both a master regulator of tumor vascularization and an oncogene in several human cancers (Feng et al., 2017; Hawkins et al., 2013). GATA2 is a hematopoietic TF, the mutation, overexpression or epigenetic dysregulation of GATA2 also mediates the tumorigenesis including acute erythroid leukemia and gastric cancer (Di Genua et al., 2020; Song et al., 2018). For SMAD4, as one of the SMADs family of signal transducer from TGF-beta, its mutation is involved in radiotherapy resistance of cancer cells (Wang et al., 2018). Besides, overexpression of SMAD4 promotes invasion and metastasis of breast cancer cells, while inhibition of SMAD4 can effectively alleviate cancer progression (Tang et al., 2017). Although the involvement of these TFs in cancer development has been noted, their effects on liver metastasis of pancreatic cancer are still undefined.

Here, we used continuously in vivo screening of the human pancreatic cancer Hs766T cell line to establish Hs766T-L3, a cell line with high liver metastatic ability. By analyzing its whole transcriptome, we revealed huge differences in gene expression patterns and pathway activation of Hs766T-L3 compared with the parental Hs766T. We correlated the difference in pathway activation with the expression of the four core TFs including STAT1, NR2F2, GATA2, and SMAD4, then examined the relative expression of these TFs in pan-cancer using the TCGA database. Among these TFs, GATA2 is considered to be involved in tumor metastasis as a potential driver. We further tested the relative effects of GATA2-mediated transcriptional activation of Notch3 on the metastatic ability of Hs766T-L3 through in vitro and in vivo experiments.

MATERIALS AND METHODS

Cells and reagents
The human pancreatic cancer cell lines Hs766T and Capan1 were obtained from the American Type Culture Collection (ATCC, USA). Hs766T was cultured with Dulbecco's modified Eagle medium (DMEM; obtained from Hyclone, USA) containing 10% fetal bovine serum (FBS; Hyclone) and 1% penicillin-streptomycin (Thermo Fisher Scientific, USA). Capan1 was cultured with Iscove's modified Dulbecco medium (IMDM; obtained from Gibco, USA) containing 20% FBS and 1% penicillin-streptomycin. Recombinant human soluble DLL1 was obtained from Enzo Life Sciences (USA). Mouse albumin ELISA kit and mouse alanine aminotransferase ELISA kit were obtained from Abcam (UK), mouse total bilirubin ELISA kit was obtained from Fusheng Industrial Co., Ltd. (China). Antibodies against NICD1 (Cat No. 3608) and NICD3 (Cat No. 2889) were purchased from Cell Signaling Technology (USA). Antibodies against β-actin (Cat No. sc-47778) was obtained from Santa Cruz Biotechnology (USA).

Animal experiments and generation of metastatic Hs766T-L3
BALB/c nude mice were obtained from the Laboratory Animal Center of Third Military Medical University (Chongqing, China). All experimental protocols were reviewed and approved by the Institutional Animal Care and Use Committee of Third Military Medical University (IACUC No. SCXK20170002). All mice were maintained under 12-h light, 12-h dark cycles and free to food and water, and the mice were euthanized according to the AVMA Guidelines for the Euthanasia of Animals. For generation of liver metastatic cancer cells, we established a pancreatic cancer spontaneous liver metastasis model. Briefly, 5×10^5 Hs766T cells stably expressed luciferase were injected into the pancreases of BALB/c nude mice. After 14 weeks, cancer cells that spontaneously metastasized to the liver were separated, expanded and reinoculated into the pancreases of next-generation recipients. After three generations of screening, the third generation of Hs766T cells (Hs766T-L3) developed liver metastasis in 9/10 mice. Hs766T-L3 cells were collected and expanded for further experiments. For evaluation of metastatic ability of cancer cells, GATA2-knockdown Hs766T-L3 and control Hs766T-L3 were injected into the pancreases of nude mice. After 6 weeks, the liver metastatic rate of cancer cells was calculated. After the mice were euthanized, the serum was isolated, and liver were harvested and weighed. The serum levels of albumin (ALB), alanine aminotransferase (ALT), and total bilirubin (TBIL) were detected according to the manufacturer's protocols.

Total RNA sequencing
Total RNA was extracted by using RNeasy mini kit (Qiagen, Germany). After that, a Qubit®2.0 Fluorometer (Life Technologies, USA) was used to detect the quality and concentration of extracted RNAs. RNA sequencing (RNA-seq) strand-specific libraries were established using the VAHTS Total RNA-seq (H/M/R) Library Prep Kit (Vazyme, China) according to the manufacturer's instructions. The library construction and sequencing were performed by Sinotech Genomics Co., Ltd.

(China). RNA-seq data has been uploaded to Sequence Read Archive (SRA) database, the BioProject ID is PRJNA734643.

Bioinformatics analysis and visualization
Data analysis and visualization were conducted using R programming language. Differentially expressed RNAs were screened with FDR adjusted P value less than 0.05 and fold change more than 2.0. As for target prediction of TFs, we used JASPAR to predict the motifs of TF binding sites (TFBSs), and these TFBSs were used to predict the TF-targeted genes by using ENCODE database. Network construction was performed in Cytoscape (ver. 3.8.1).

Bioluminescence imaging
First, mice were injected intraperitoneally with D-Luciferin, sodium salt at a concentration of 10 µl/g body weight. Then mice were anesthetized with 1.5% concentrations of isoflurane. Ten minutes later, place the sample in the center of the imaging platform and proceed according to the operating instructions.

Proliferation, migration, and invasion assay of cancer cells
We performed CCK8 assay to measure the proliferation of cancer cells. Briefly, 5×10^3 Hs766T-L3 and GATA2-knockdown Hs766T-L3 cells were seeded in a 96-well plate. Cell proliferation was detected at 1, 2, and 3 days after culture using CCK8 kit. To detect the migration of cancer cells, wound healing assay was performed. Hs766T-L3, GATA2-knockdown Hs766T-L3 cells and Notch3-knockdown Hs766T-L3 cells were seeded in the plates, respectively. When cells adhere to the plates, use a pipette tip to make a scratch like an incision-like gap. After incubation for 24 h, the healing was observed and wound healing efficiency is quantified. Cell invasion was measured a 24-well transwell chamber with a pore size of 8 µm (Corning Life Sciences, USA). Hs766T-L3, GATA2-knockdown Hs766T-L3 cells and Notch3-knockdown Hs766T-L3 cells were re-suspended in serum-free medium and seeded in the upper chamber coated with Matrigel matrix, respectively. On the lower chamber, medium with 20% FBS was added. After incubation for 24 h, crystal violet staining was used and the number of invaded cells was quantified.

Transfection of lentivirus
Lentiviral shRNA constructs of GATA2 and Notch3 were obtained from Genechem Co., Ltd., China. For lentivirus transfection, 5×10^3 Hs766T-L3 cells were seeded in a 24-well plate. When cells made a confluence of 30%-40%, cell's transfection was performed according to the manufacturer's recommendations. After transfection for 24 h, medium containing 5 µg/ml puromycin solution was replaced until stable cells expressing the shRNA were screened out.

Flowcytometry
For apoptosis detection, Annexin V/PI Apoptosis Detection Kit was used to detect the apoptosis rate after knockdown of GATA2. 5×10^5 cells were harvested and washed with phosphate-buffered saline. Then cells were re-suspended with 100 µl binding buffer. Add 5 µl Annexin V-FITC and 10 µl PI

staining solution and gently mix. Keep the sample at dark and incubated at room temperature for 10 min. After incubation, all samples were measured by a flow cytometer (Beckman, USA), and the data were analyzed by FlowJo software (FlowJo LLC, USA).

Real-time quantitative polymerase chain reaction
Total RNA was extracted using RNAiso Plus Reagent (Takara Bio, Japan). PrimeScript Real-Time Reagent Kit (Takara Bio) was used to prepare RNA into cDNA according to the operating instructions. SYBR Premix Ex Taq II (Takara Bio) was used for real-time polymerase chain reaction (PCR). The Real-time quantitative PCR (RT-qPCR) primer sequences were listed in the Supplementary Table S1. β-Actin were used as internal control.

Western blot analysis
Protein was isolated from Hs766T-L3 cells using lysis buffer (Beyotime Biotechnology, China) containing 1% protease inhibitors. Then denatured protein samples were subjected to SDS–PAGE for electrophoresis. Next, the proteins were transferred onto polyvinylidene fluoride (PVDF) membrane (Millipore, USA). After blocking in 5% skim milk at room temperature for 2 h, membranes were incubated with primary antibodies against NICD3 (1:1,000; Cell Signaling Technology), NICD1 (1:1,000; Cell Signaling Technology), and Actin (1:2,000; Santa Cruz Biotechnology) overnight at 4°C. After washing with TBST for three times, the membranes were incubated with appropriate secondary antibodies at 37°C for 2 h. High Sensitivity ECL kit was used to detect chemiluminescent signals.

Chip assay
ChIP was performed using the ChIP express kit (Millipore). Briefly, cells were fixed with 1% formaldehyde for 10 min. Immunoprecipitation was done with anti-GATA2 and anti-IgG antibodies. The bound DNA fragments were purified using spin columns and amplified with Notch1 or Notch3 promoter-specific primers. The primer sequences used in ChIP detection are also shown in Supplementary Table S1.

Statistical ananlysis
All data were collected and expressed as mean ± SD. Prism 6 software (GraphPad Software, USA) was used for data analysis. We use two-sided t-tests for comparing two sets of data and one-way ANOVA for comparing multiple sets of data, respectively. $P < 0.05$ and $P < 0.01$ were considered statistically significant.

RESULTS

Generation of liver metastatic Hs766T-L3
In this study, we used two human pancreatic cancer cell lines Capan1 and Hs766T to obtain pancreatic cancer cells with high metastatic ability. Tumor cells stably expressed luciferase were injected into the pancreases of BALB/c nude mice. After 14 weeks, tumor cells that spontaneously metastasized to the liver were separated, expanded and reinoculated into the pancreases of next-generation recipients. Only Hs766T

successfully developed spontaneous liver metastases after six-week inoculation. The liver metastatic rate of each generation of Hs766T was measured, and the results showed that this rate increased with the addition of generations (Fig. 1A). Notably, the liver metastatic rate of the parental Hs766T was 20% (2/10 mice), while that of the third generation of Hs766T (Hs766T-L3) increased to 90% (9/10 mice). After 6 weeks of injection, bioluminescence imaging (BLI) analysis showed that Hs766T-L3 induced obvious liver metastases (Fig. 1B). Then, mice were euthanatized and the liver/body mass ratio was measured. The liver weight of mice inoculated with Hs766T-L3 was significantly higher than the parental Hs766T, with diffuse tumor lesions throughout the liver (Fig. 1C). H&E staining showed that the histological structure of livers was destroyed by tumor colonies in the Hs766T-L3 group, whereas livers of mice inoculated with the parental
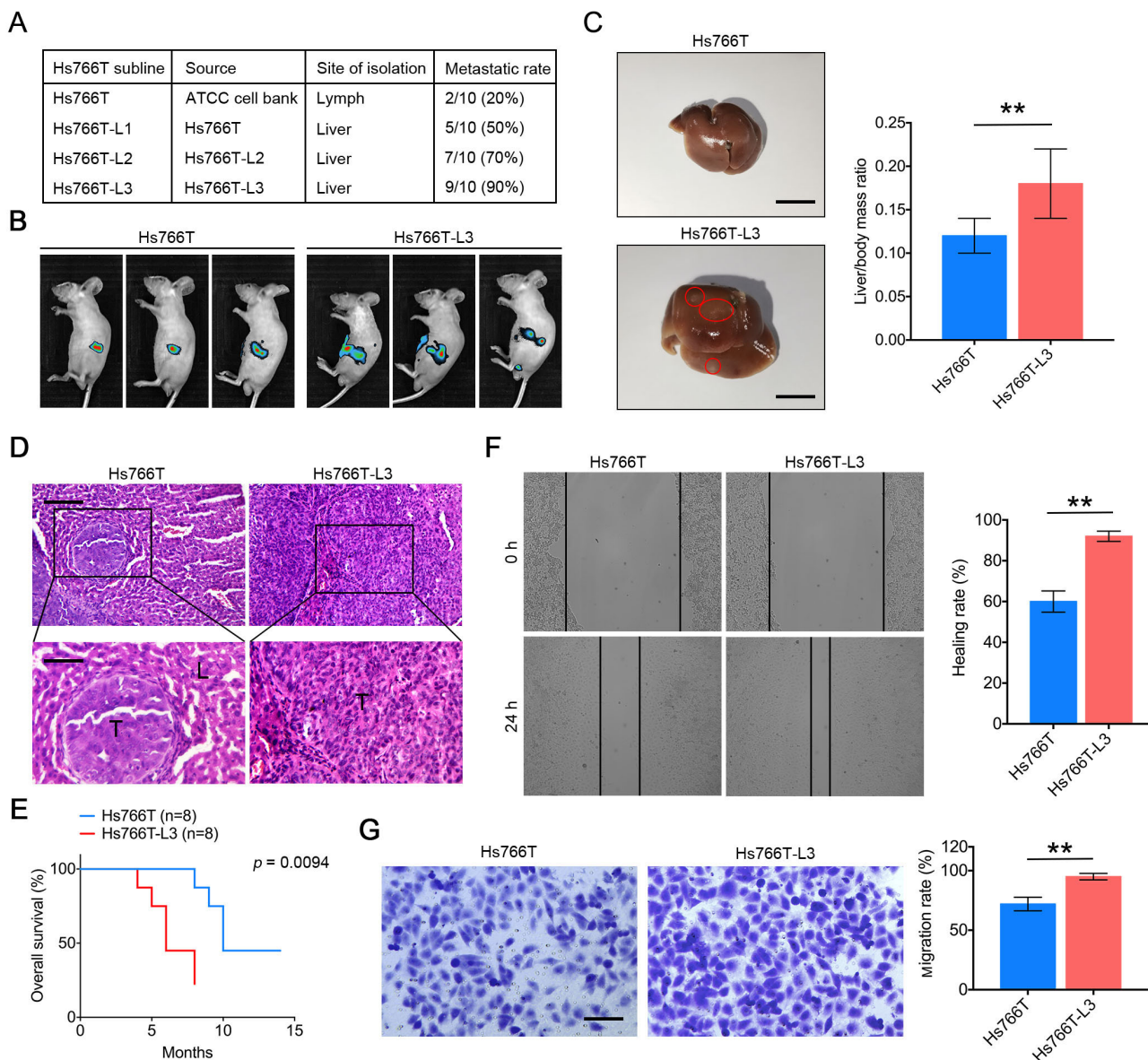

Fig. 1. Generation of liver metastatic Hs766T-L3. (A) Incidence of spontaneous metastasis to the liver generated by parental cells and various Hs766T sublines. (B) Representative BLI images showed the liver metastatic progression of Hs766T-L3 and the parental Hs766T. n = 10 per group. (C) Gross examination of liver metastasis induced by Hs766T and Hs766T-L3 in BALB/c nude mice. Scale bars = 1 cm. (D) H&E staining of metastatic foci after intra-splenic injection of Hs766T and Hs766T-L3 in nude mice. Scale bars = 300 μm (upper); 100 μm (bottom). (E) Kaplan-Meier survival analysis of mice from three treatment group, n = 8. (F) Hs766T and Hs766T-L3 were seeded into the lower chamber until complete fusion, then the scratch was generated. After 24 h, the scratch was observed and the healing rate was calculated. n = 3 per group. (G) Hs766T and Hs766T-L3 were seeded into the transwell upper chamber, and FBS were added into the lower chamber. After 24 h, cell migration was examined. Scale bar = 50 μm. n = 3 per group. The results are presented as the mean ± SEM. **$P < 0.01$.

Hs766T retained a relatively integral structure with significantly reduced metastatic lesions (Fig. 1D). Besides, Hs766T-L3 mice showed a reduced overall survival compared with that of mice inoculated with Hs766T (Fig. 1E). We then assessed the proliferation, migration, and invasion ability of Hs766T-L3 through *in vitro* experiments. The wound healing assay revealed that the wound had nearly healed in the Hs766T-L3 group at 24 h after scratching, compared with a 60% healing efficiency in the Hs766T group (Fig. 1F). The migrated cell number of the Hs766T-L3 group through transwell chambers was also significantly greater than the parental Hs766T cells (Fig. 1G). So far, after three consecutive generations of selection and expansion, we obtained highly invasive and metastatic Hs766T-L3 compared with the parental Hs766T.

Transcriptomic profiling of liver metastatic Hs766T-L3

To establish the transcriptomic profiling of Hs766T-L3 and its parental cell line Hs766T, we extracted RNA samples from Hs766T-L3 and Hs766T and performed RNA-seq using an Illumina NovaSeq 6000. Each differentially expressed RNA is statistically significant ($P < 0.05$), and the fold change is greater than 2.0. In total, 2445 messenger RNAs (mRNAs), 244 microRNAs (miRNAs), 257 long non-coding RNAs (lncRNAs), and 83 circular RNAs (circRNAs) were differentially upregulated, while 2749 mRNAs, 236 miRNAs, 289 lncRNAs, and 49 circRNAs were differentially downregulated in Hs766T-L3 compared with Hs766T (Fig. 2A). Clustering heatmaps presented the top 40 RNAs differentially expressed in this comparison group (Fig. 2B). lncRNA plays critical roles
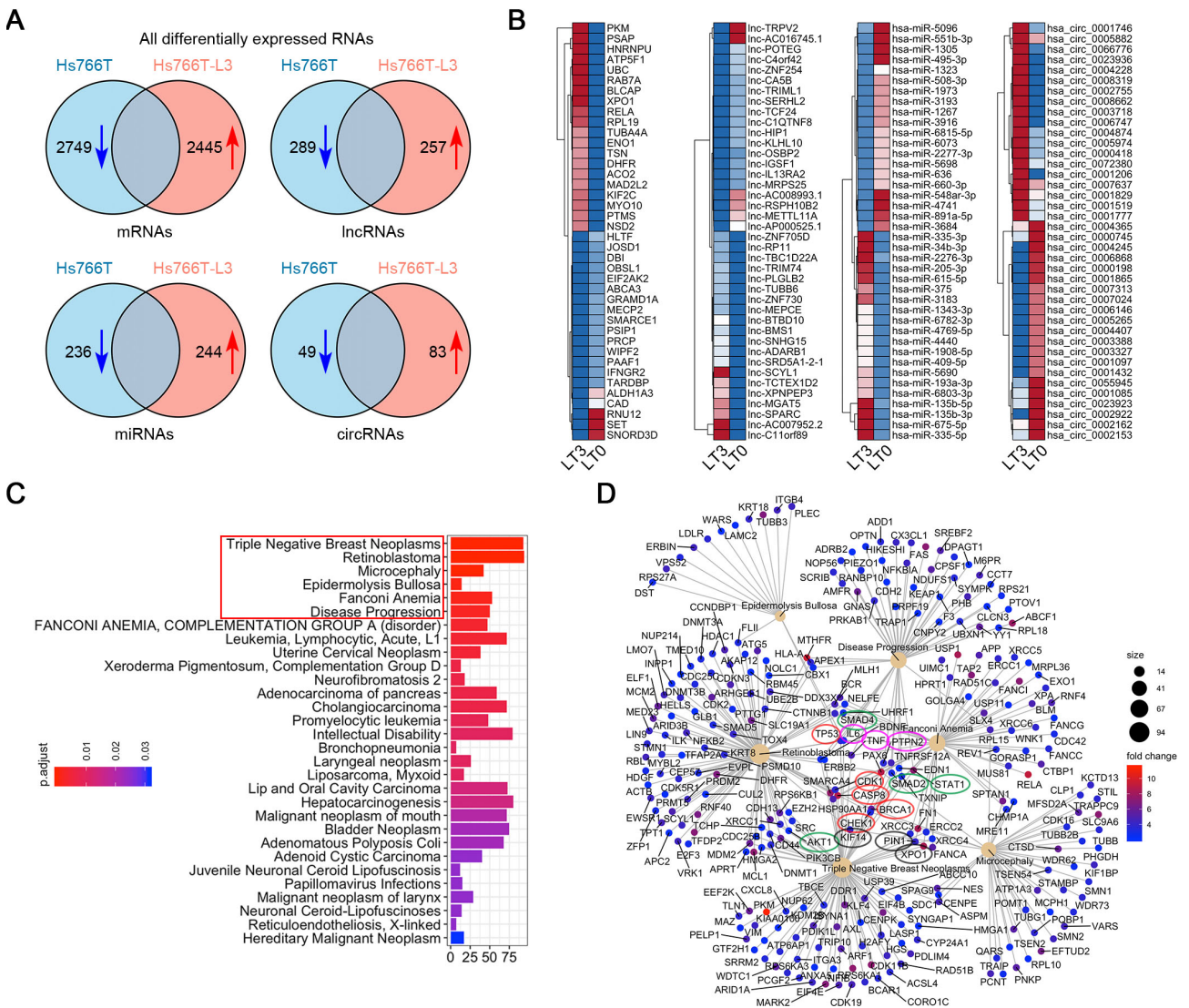

Fig. 2. Transcriptomic profiling of liver metastatic Hs766T-L3. (A) The number of upregulated and downregulated RNAs in Hs766T-L3 was shown in Venn plots. The red arrow represents upregulated RNAs, and the blue arrow represents downregulated RNAs. (B) Clustering heatmaps showed the top 40 RNAs differentially expressed Hs766T-L3 and Hs766T. (C) Disease-related enrichment analysis of upregulated mRNAs in Hs766T-L. The red box circles the top six most significant items. (D) Genes involved in the top six significant disease-related terms were mapped through a gene-concept network.

in cancer progression via serving as competing endogenous RNA (ceRNA) to hinder the miRNA involvement in posttranscriptional regulatory networks in tumor cells (Karreth and Pandolfi, 2013). *In silico* analysis was performed to predict the lncRNA-targeted miRNAs and the miRNA-targeted mRNAs, and the top four differentially upregulated lncRNAs in Hs766T-L3 was selected to construct a ceRNA network. In total, 40 interactions between 4 lncRNAs and 19 miRNAs were identified and 291 interactions between 19 miRNAs and 219 mRNAs were identified (Supplementary Fig. S1). To explore the correlations between differentially upregulated genes in Hs766T-L3 and diseases, we performed a disease-related enrichment analysis using DisGeNET, an integrative and comprehensive resource of gene-disease associations. The results showed that this cluster of genes that upregulated in Hs766T-L3 is closely associated with the occurrence and progression of various cancers, including triple negative breast cancer, retinoblastoma, leukemia, cervical cancer and pancreatic cancer (Fig. 2C). The top six enriched items of disease were selected, and specific genes involved in these terms were mapped through a gene-concept network (Fig. 2D). A variety of genes known to be involved in the regulation of cancer progression were identified in the network center, including cell cycle regulators (TP53, CDK1, CASP8, BRCA1, CHEK1), signal cascade molecules (SMAD2/4, STAT2, AKT1), and molecules involved in tumor immunity (IL6, TNF, PTPN). In addition, several molecules such as KIF14, PIN1 and XPO1 were reported to play critical roles in the initial activation and driving of tumors, and they are key therapeutic targets (Singel et al., 2013; Zhou and Lu, 2016).

Mapping the characteristic gene expression patterns of Hs766T-L3

We used gene set enrichment analysis (GSEA) to investigate the expression patterns of genes in Hs766T-L3 in predefined gene sets of gene ontology. Two hundred and fifty gene sets were significantly expressed (FDR < 0.25) between two phenotypes of Hs766T-L3 and Hs766T, of which 51 gene sets were significantly upregulated and 19 gene sets were significantly downregulated. The top 30 upregulated gene sets were presented (Fig. 3A). We performed functional similarity analysis of all upregulated gene sets and discovered that these gene sets were highly correlated with several types of biological process (BP) including cell cycle, cell catabolism, immune response and cytoskeleton organization, indicating the unique gene expression patterns of Hs766T-L3, which may lead Hs766T-L3 plays distinctive roles in specific situations (Fig. 3B). We further used GSEA plots to rank and score the genes involved in the top two significant items of each type of BP items. Accordingly, the top 20 core enriched genes involved in corresponding BP terms were shown as clustering heatmaps (Fig. 3C). Specifically, the core enriched genes of two cell cycle-related items, 'cell cycle phase transition (GO:0044770)' and 'cell cycle process (GO:0022402)', were mainly composed of a group of cell cycle regulators such as CDK2, BRCA1, and CDC45 (Deng, 2002; Leatherwood, 1998). The genes involved in the regulation of cell energy metabolism including ENO1, PLK2, and PTK2 were defined as the core enriched genes of cell catabolism (Cappello et al.,

2018; Roy-Luzarraga and Hodivala-Dilke, 2016; Strebhardt, 2010). Genes play critical roles in tumor escape and immunosuppression including TNIP1, ADAM15 and SHMT2 were defined as the core enriched genes of 'innate immune response (GO:0045087)' and 'regulation of immune response (GO:0050776)' (Ahmed et al., 2013; Sukhov et al., 2016; Walden et al., 2019). Genes involved in the cytoskeletal reorganization including MARK2, DNTN1, and RAB7A (Cogli et al., 2013; Lin et al., 2009; Rosas-Salvans et al., 2019), were defined as the core enriched genes of 'regulation of organelle organization (GO:0033043)' and 'regulation of cytoskeleton organization (GO:0051493)'. Besides, we also performed Gene ontology and KEGG analysis of all differentially upregulated genes in Hs766T-L3, and the results are partially consistent with GSEA (Supplementary Fig. S2). Together, these findings suggest that Hs766T-L3 possesses distinctive patterns of gene expression, contributing to the striking differences between Hs766T-L3 and the parental Hs766T in cell cycle regulation, energy metabolism, immunoregulation and cytoskeleton organization.

Identification of pathways and transcriptional factors involved in metastasis of Hs766T-L3

To explore the pathways involved in the invasion and metastasis of pancreatic cancer, we performed Reactome GSEA to identify the signaling pathways specifically activated in Hs766T-L3. In total, 279 pathways were significantly expressed (FDR < 0.25) between two phenotypes of Hs766T-L3 and Hs766T, of which 258 pathways were significantly upregulated and 21 pathways were significantly downregulated. The top 34 upregulated pathways were presented (Fig. 4A). The upregulated pathways are mainly composed of signaling pathways associated with interleukin family, toll like receptors (TLRs) and Notch family. Genes involved in the top six significant upregulated pathways were ranked and scored, with a clustering heatmap showing the core enriched genes (Figs. 4B and 4C). The high ranking of these pathways indicates the potential involvement of these core enriched genes in metastasis of Hs766T-L3. TFs are closely involved in the development of cancers through governing the activation status of downstream signaling. We noticed that several TFs were located in the core enriched genes, including STAT1, SMAD4, NR2F2, and GATA2. We further used JASPAR database to predict the TFBSs of these TFs, which are highly conserved among species (Fig. 4D). These TFBSs were used to efficiently predict the TF-targeted genes, and a network mapping the interactions between 4 TFs and 153 TF-targets genes were visualized (Fig. 4E). The dense interactions between TFs and target genes indicate that these TFs coordinately regulate the BP related to the growth and progression of tumor cells, including drug resistance, immune regulation and cellular energy metabolism.

The relationships between the expression of TFs in pan-cancer and prognosis

We analyzed the relative expression of the four TFs in multiple cancers through combining the sequencing data of clinical tumor samples from The Cancer Genome Atlas (TCGA). Eight types of cancer were divided into four epithelial cancers
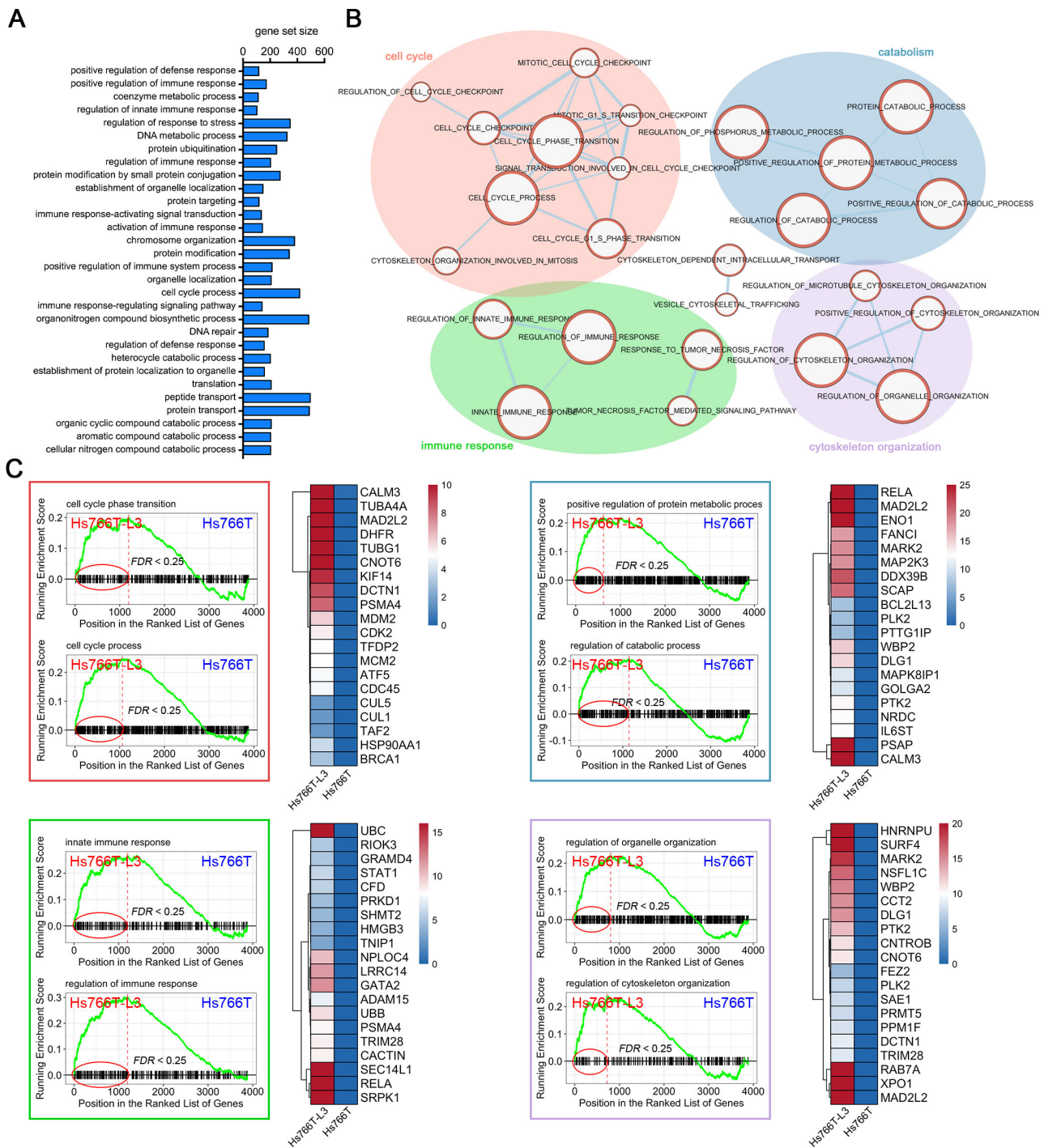
Fig. 3. Mapping the characteristic gene expression patterns of Hs766T-L3. (A) The top 30 upregulated gene sets of Hs766T-L3 from GSEA analysis were presented. (B) An enrichment map showed that upregulated gene sets in Hs766T-L3 were closely correlated with cell cycle, cell catabolism, immune response and cytoskeleton organization. (C) GSEA enrichment plots of representative gene sets. The top 20 core enriched genes involved in corresponding gene sets were shown as clustering heatmaps.

and four non-epithelial cancers according to the different tissue sources of tumor cells, and the relative expression of TFs in these cancers were analyzed (Fig. 5A). We discovered that STAT1 was overexpressed in both epithelial cancers and non-epithelial cancers, while NR2F2 was overexpressed in

pancreatic adenocarcinoma (PAAD) of epithelial cancers, and glioblastoma multiforme (GBM) and lymphoid neoplasm diffuse large B-cell lymphoma (DLBC) of non-epithelial cancers. SMAD4 was not overexpressed in four non-epithelial cancers while overexpressed in large acute myeloid leukemia (LAML)
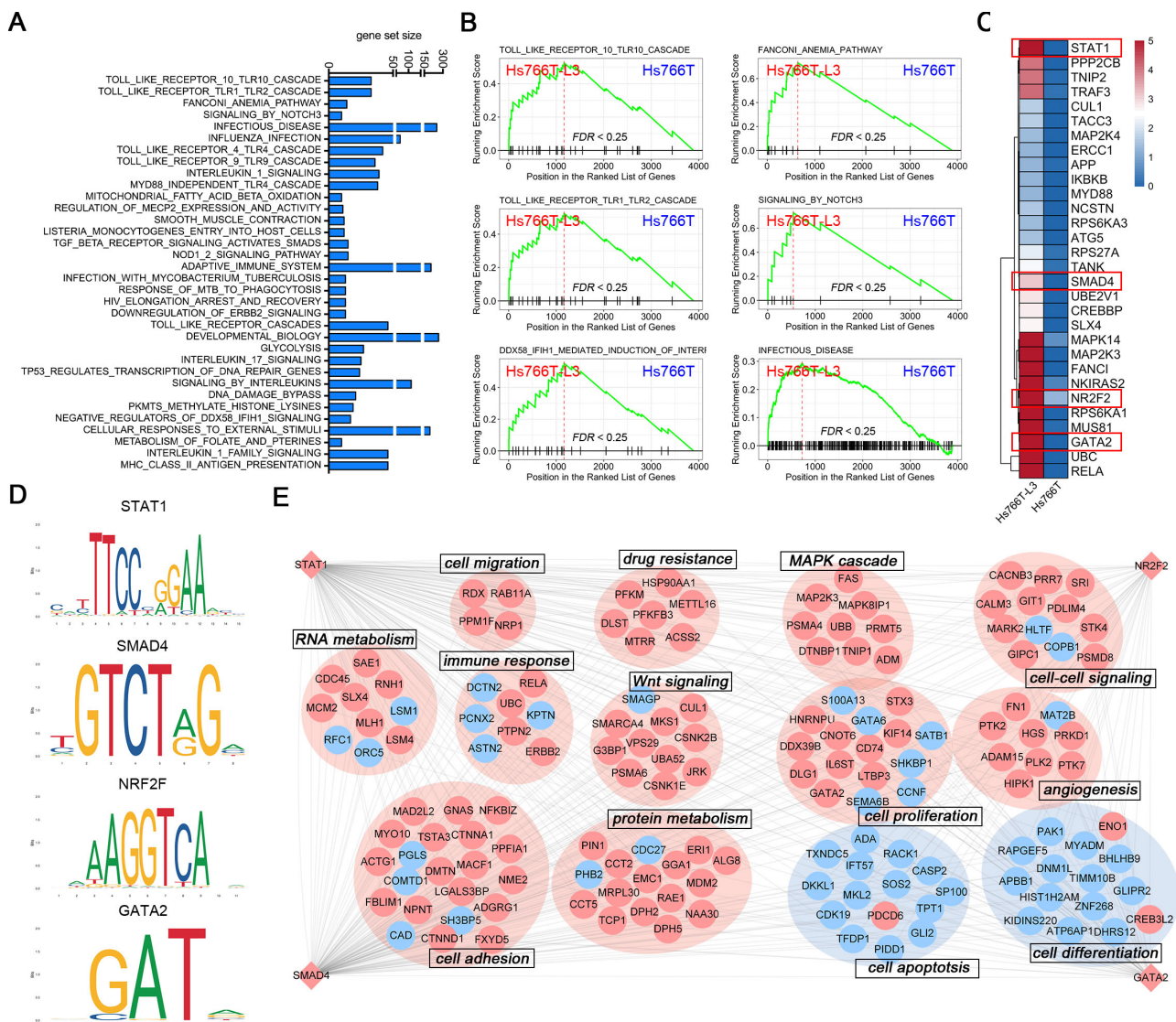
Fig. 4. Identification of pathways and transcriptional factors involved in metastasis of Hs766T-L3. (A) The top 34 upregulated pathways of Hs766T-L3 from Reactome GSEA analysis were presented. (B) GSEA enrichment plots showed the top six significant upregulated pathways. (C) Genes involved in the top six significant upregulated pathways were shown as clustering heatmaps. (D) The sequence motif of TFBSs with highly conserved among species was predicted through JASPAR database. (E) A network model showing the relationships between the TFs and their targets. The nodes with the same BPs were grouped into the same modules, each of which was named according to the corresponding BP terms. Red and blue node colors represent upregulation and downregulation of the genes in Hs766T-L3. Diamond and circle nodes denote TFs and their target genes of transcriptional regulation. Red and blue background colors denote the BPs represented by (1) upregulated genes in Hs766T-L3 and targets of the TFs, and (2) downregulated genes in Hs766T-L3 and targets of the TFs.

and GBM of non-epithelial cancers. The expression of GATA2 was not increased in all the eight cancers compared with normal tissues. We further used Kaplan–Meier survival analysis to assess the relationships between the expression of TFs and the prognosis of patients with pancreatic cancer. In consistency, the overexpression of STAT1 or NR2F2 was associated with a poor survival of patients, while the expression pattern of SMAD4 is not significantly correlated with the overall survival. Intriguingly, although the expression of GATA2 is not significantly upregulated in tumor tissues, the overexpression

of GATA2 in pancreatic cancer is closely correlated with the poor survival rate of patients (Fig. 5B). We further studied the expression alterations of TFs with the progression of the clinicopathological stage stages of pancreatic cancer, and discovered a consistently upregulation of GATA2 during progression of pancreatic cancer (Fig. 5C). These results indicate that GATA2 may play regulatory roles in a relative late stage during tumor progression.
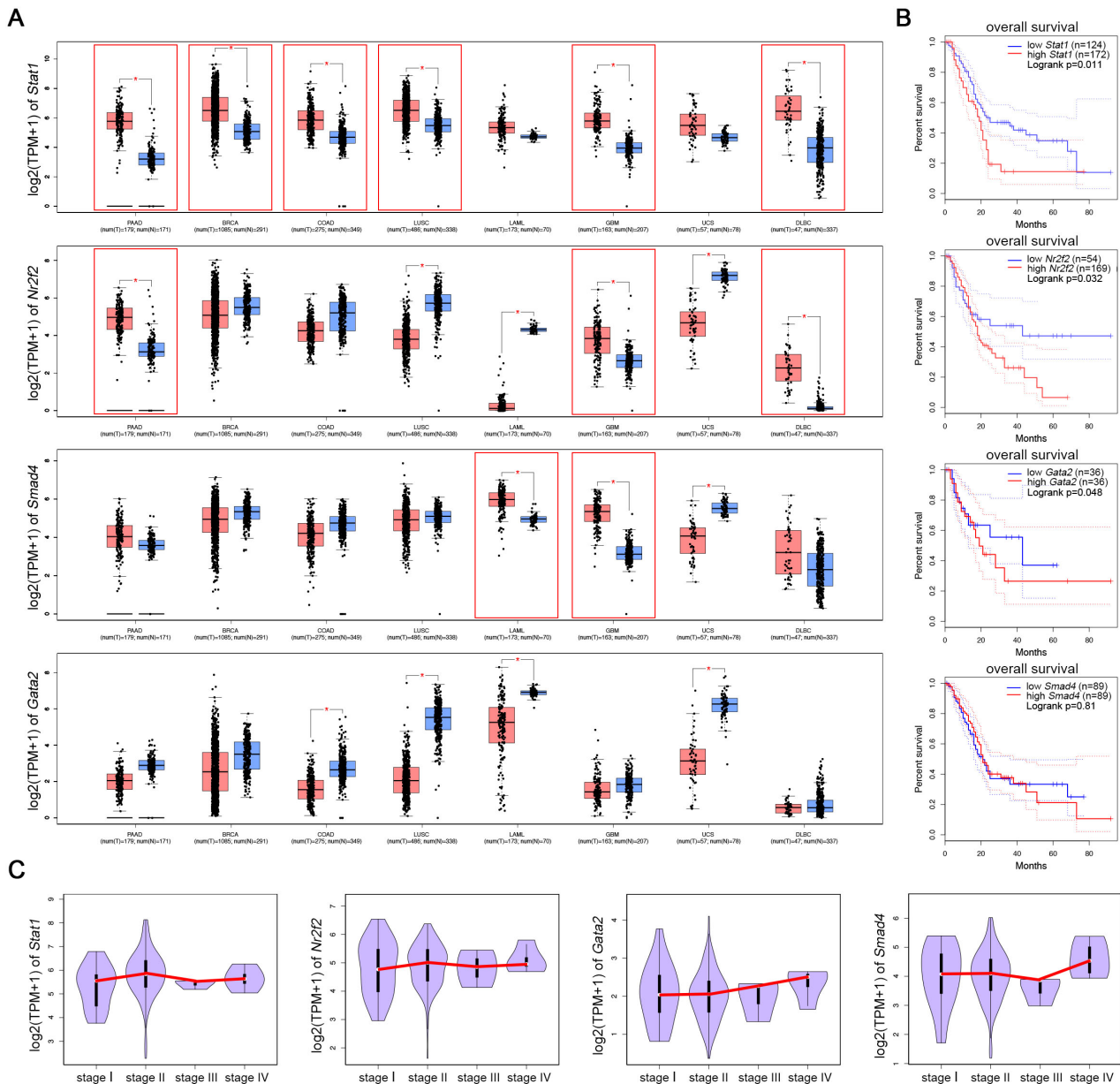
Fig. 5. The relationships between the expression of TFs in pan-cancer and prognosis. (A) The relative expression of Stat1, Nr2f2, Smad4, and Gata2 in four types of epithelial cancers and four types of non-epithelial cancers. The red box indicates that TF is significantly upregulated in this type of cancer. Epithelial cancers include pancreatic adenocarcinoma (PAAD), breast invasive carcinoma (BRCA), prostate adenocarcinoma (PRAD), and lung squamous cell carcinoma (LUSC). Non-epithelial cancers include lymphoid neoplasm diffuses large B-cell lymphoma (DLBC), large acute myeloid leukemia (LAML), uterine carcinosarcoma (UCS), and glioblastoma multiforme (GBM). $*P < 0.05$. (B) Kaplan-Meier survival analysis showed the correlations between the expression level of TFs and the prognosis of patients with pancreatic cancer. (C) Violin plots showed the expression alteration of TFs with the progression of the clinicopathological stage stages of pancreatic cancer.

Knockdown of GATA2 inhibits the liver metastasis of Hs766T-L3 and preserves liver function

To explore whether GATA2 is involved in the liver metastatic progression of Hs766T-L3, GATA2 was knockdown in Hs766T-L3 using lentivirus transfection system and transfection efficiency was confirmed (Supplementary Fig. S3A).

We tested the proliferation, migration, and invasion of GATA2-knockdown Hs766T-L3 in vitro, the results showed that knockdown of GATA2 had no significant effects on cell proliferation, while it markedly reduced the invasion and migration ability of Hs766T-L3 (Figs. 6A-6C). No significant changes in apoptosis rate were observed after knockdown of GATA2
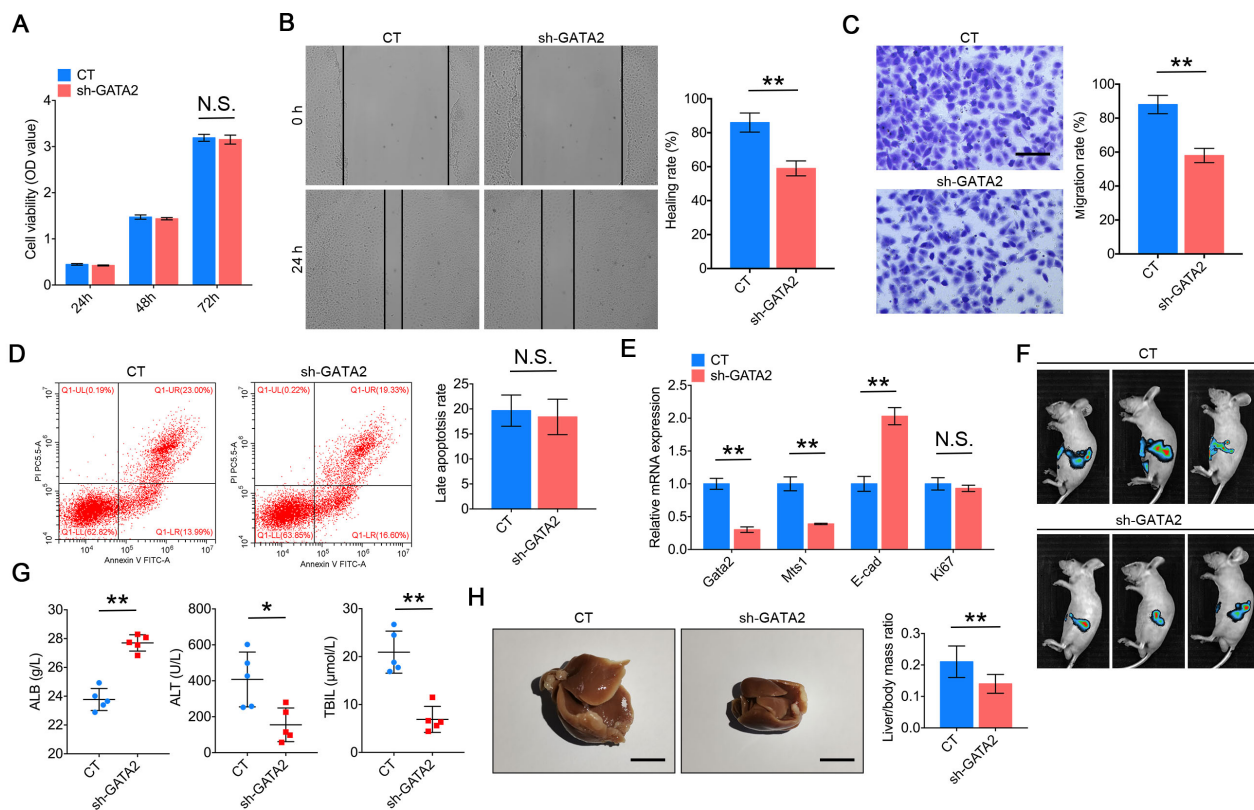
Fig. 6. Knockdown of GATA2 inhibits the liver metastasis of Hs766T-L3 and preserves liver function. (A) The proliferation of Hs766T-L3 after GATA2 knockdown was detected at 24, 48, and 72 h. CT, control. (B) After GATA2 knockdown, Hs766T-L3 were seeded into the lower chamber until complete fusion, then the scratch was generated. After 24 h, the scratch was observed and the healing rate was calculated. n = 3 per group. (C) After GATA2 knockdown, Hs766T-L3 were seeded into the transwell upper chamber, and FBS were added into the lower chamber. After 24 h, cell migration was examined. Scale bar = 50 μm. n = 3 per group. (D) Annexin V/PI analysis examined the apoptosis of GATA2-knockdown Hs766T-L3. n = 3 per group. (E) Relative mRNA expression of Gata2, Mts1, E-cad, and Ki67 of Hs766T-L3 after knockdown GATA2. (F) Representative BLI images showed the liver metastatic progression of Hs766T-L3 knockdown GATA2. n = 5 per group. (G) Concentration of the mouse serum liver function markers ALB, ALT, and TBIL after six weeks of Hs766T-L3 injection. (H) Gross examination of liver metastasis induced by GATA2-knockdown Hs766T-L3 in BALB/c nude mice. Scale bars = 1 cm. The results are presented as the mean ± SEM. *P < 0.05; **P < 0.01; N.S., not significant.

(Fig. 6D). Consistently, we also performed RT-qPCR analysis for validation at the mRNA level. After knockdown of GATA2, the mRNA expression of metastasis-related gene *Mts1* (also known as *Metastasin1*) was decreased and the mRNA expression of epithelial cadherin (*E-cadherin*) was upregulated, suggesting a reduction in invasiveness of Hs766T-L3 (Fig. 6E). The expression of proliferation-related gene *Ki67* did not alter significantly after knockdown of GATA2. These results indicated that GATA2 might serve as an important regulator mediating the migration and invasion of Hs766T-L3. We further inoculated GATA2-knockdown Hs766T-L3 into the pancreases of nude mice. Intriguingly, knockdown of GATA2 alleviated the metastatic burden and progression, as confirmed by BLI (Fig. 6F). After six-week normal breeding, three liver function markers of mice TBIL, ALT, and ALB were tested, and the results showed that three indicators have altered significantly after knockdown of GATA2 (Fig. 6G). In addition, the liver metastatic rate of GATA2-knockdown Hs766T-L3 reduced to 50% (5/10 mice), and the liver weight of mice was significantly reduced compared with the control group (Fig.

6H). Together, the above data indicates the critical roles of GATA2 in regulating liver metastasis of Hs766T-L3.

GATA2 regulates the transcriptional activity of Notch3 to promote invasion and metastasis of Hs766T-L3

Aberrant activation of Notch3 signaling contributes the metastatic progression of several cancers (Inder et al., 2017; Screpanti et al., 2003). Intriguingly, *in silico* prediction also identified Notch3 as a potential target for transcriptional regulation of GATA2. We therefore sought to explore whether GATA2 and Notch3 coordinately regulate the invasion and metastasis of Hs766T-L3. Our RNA-seq data showed that both *Notch3* and *Gata2* were highly expressed in Hs766T-L3, which were also confirmed by RT-qPCR analysis (Fig. 7A). We constructed Notch3-knockdown Hs766T-L3 cells through lentivirus transfection system (Supplementary Fig. S3B). Knockdown of Notch3 significantly inhibited the migration and invasion ability of Hs766T-L3, characterized by the reduced wound healing efficiency and migrated cell number through the transwell chambers (Figs. 7B and 7C). Besides, the expression
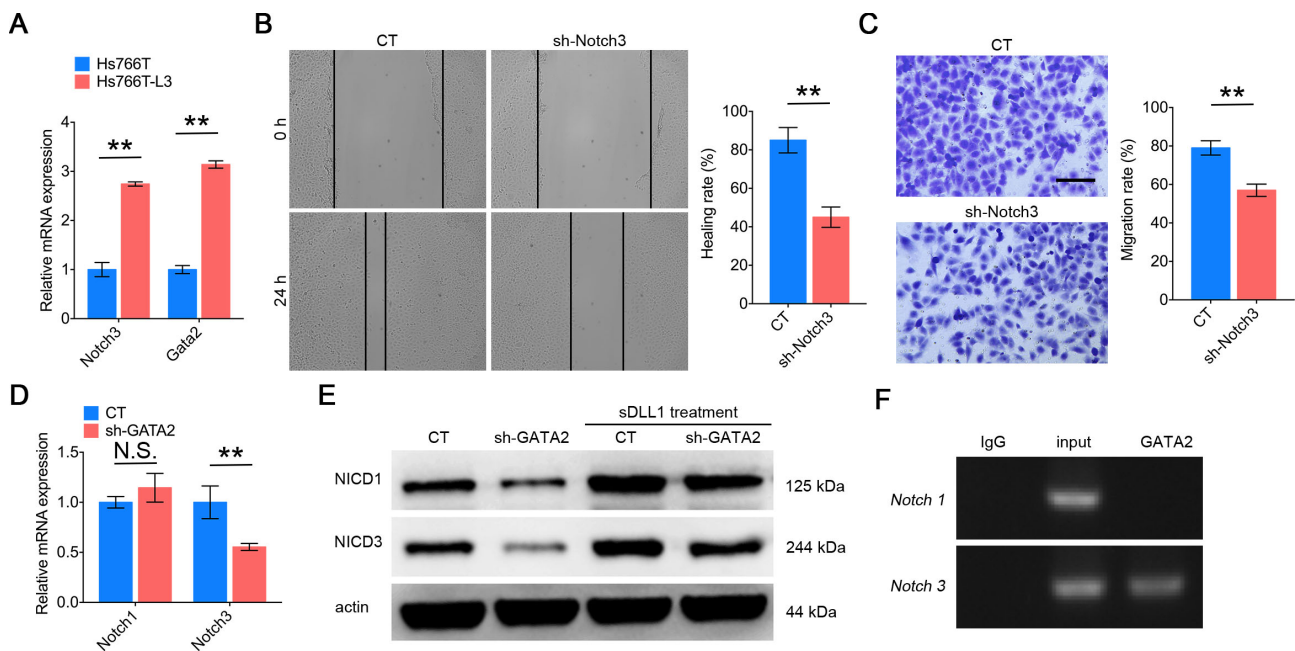
Fig. 7. GATA2 regulates the transcriptional activity of Notch3 to promote invasion and metastasis of Hs766T-L3. (A) Relative mRNA expression of Notch3 and Gata2 in Hs766T and Hs766T-L3. (B) After Notch3 knockdown, Hs766T-L3 were seeded into the lower chamber until complete fusion, then the scratch was generated. After 24 h, the scratch was observed and the healing rate was calculated. n = 3 per group. CT, control. (C) After Notch3 knockdown, Hs766T-L3 were seeded into the transwell upper chamber, and FBS were added into the lower chamber. After 24 h, cell migration was examined. Scale bar = 50 μm. n = 3 per group. (D) Relative mRNA expression of Notch1 and Notch3 in Hs766T-L3 after knockdown GATA2. (E) Western blots of NICD1 and NICD3 in sDLL1-treated Hs766T-L3. (F) Chip assay showed the binding of GATA2 to the promoter of Notch3. The results are presented as the mean ± SEM. **$P <$ 0.01; N.S., not significant.

of *Notch3* was downregulated after knockdown of GATA2, while the expression of *Notch1* showed no obvious change (Fig. 7D). As a classical ligand of Notch signaling, delta-like1 (DLL1) are closely involved in the progression of various cancers (Takebe et al., 2014). Application of soluble DLL1 (sDLL1) simultaneously activate the signaling pathway of Notch1 and Notch3, characterized by the increasing protein level of intracellular domain of Notch1 (NICD1) and Notch3 (NICD3). However, knockdown of GATA2 abrogated the upregulation of NICD3 instead of NICD1 (Fig. 7E). Chip assay further confirmed the specific binding of GATA2 to the promoter regions of Notch3 instead of Notch1 (Fig. 7F). Together, these results suggest the specific transcriptional activation of GATA2 to Notch3, which mediates the invasion and metastasis of Hs766T-L3.

DISCUSSION

Cancer cell populations established from patients with advanced disease are heterogeneous, comprising distinctive genomic characteristics and metastatic abilities (Kang et al., 2003). Recent years, *in vivo* selection has been proved as an effective way in separating highly metastatic subpopulations from the parental cell lines (Clark et al., 2000). Thus, we used similar approach to identify and select the subpopulations of Hs766T-L3 with the capacity to home and colonize at liver. A previous study showed that the metastatic capacity of cancer

cells is closely associated with distinctive genomic expression profiles (Kang et al., 2003). They also found that the expression of several genes including IL-11, MMP-1, CTGF, and CXCR-4 is specifically upregulated in highly metastatic subpopulations of breast cancer cells. In consistency, we also revealed huge differences in expression profile of Hs766T-L3 compared with the parental Hs766T. The most prominently overexpressed genes in Hs766T-L3 encode proteins that regulate the cell cycle, catabolism and immune response, each of them with functions that may alter the cell behaviors to better adapt to external stimuli, such as cellular immunity and drug therapy. Studies have suggested that signaling associated with TLRs, interleukins and Notch receptors are involved in the tumorigenesis and cancer development (Alvarado et al., 2017; Angkasekwinai and Dong, 2021; Hennessy et al., 2010; Jones and Jenkins, 2018; Meurette and Mehlen, 2018; Radtke et al., 2013). Similarly, we discovered that the prominently activated pathways in Hs766T-L3 also include signaling mediated by TLR-1, TLR-2, TLR-4, TLR-9, TLR-10, IL-1, and Notch3. The coordinated activation of these signaling pathways might mediate the alterations in tumor behaviors, including proliferation, apoptosis, metastasis, immune escape and drug resistance.

Abnormal regulation of TFs plays essential roles in cancer progression. In this study, we identified the TF GATA2 as a potential metastatic driver of pancreatic cancer Hs766T-L3. GATA2 was initially found to be closely involved in the ho-

meostatic maintaining of hematopoiesis, lymph and immune system (Hahn et al., 2011; Spinner et al., 2014). In recent years, increasing studies have shown that GATA2 mediates the tumorigenesis and development of diverse cancers. A study reported that GATA2 is upregulated during the progression of lethal prostate cancer and contributes to the aggressive properties of cancer (Vidal et al., 2015). Specifically, GATA2 promotes the transcriptional activity of IGF and the activation of its downstream AKT, JNK and ERK1/2 to regulate chemotherapy resistance and tumorigenesis of prostate cancer (Vidal et al., 2015). Similarly, GATA2 inhibits the expression of MHC class I chain-related protein A/B (MICA/B) via binding their promoters, thereby mediating cancer cells to escape from immune surveillance (Duan et al., 2019). By contrast, loss of GATA2 expression inhibits cancer proliferation and induces chemotherapy-mediated apoptosis in acute myeloid leukemia (Menendez-Gonzalez et al., 2019). However, the roles of GATA2 in cancer metastasis has not been clearly illustrated. In this study, we aimed to find potential molecules that regulate cancer metastasis and corresponding mechanisms, laying the foundation for searching new therapeutic targets or prognostic biomarkers for liver metastasis of pancreatic cancer. We found that compared with the parental Hs766T, GATA2 was upregulated in metastatic Hs766T-L3 and its expression was closely associated with multiple signaling pathways that activated in Hs766T-L3. Further in vitro and in vivo experiments showed that GATA2 serve as a critical regulator mediating the liver metastasis of Hs766T-L3, knockdown of GATA2 impairs the metastatic ability of Hs766T-L3 while did not significantly affect the cell proliferation. These findings suggest that GATA2 may play diverse roles in different cancer cells.

Several studies have revealed the diverse interactions between GATA family and Notch signaling. Notch1-mediated RBP-J activation increased the expression of GATA2, as a critical event for the onset of definitive hematopoiesis in the embryo (Robert-Moreno et al., 2005). The competition and collaboration between GATA3 and Notch signaling also regulate the early fate determination of T cells (Rothenberg and Scripture-Adams, 2008). Notably, a recent study suggested that activation GATA2-mediated Notch signaling suppresses myelopoiesis, while absence of GATA2 fails to suppress commitment to the myeloid fate (de Pooter et al., 2006). Notch signaling has been reported to be involved in tumor angiogenesis and metastasis (Garcia and Kandel, 2012). However, few studies have focused on revealing the interaction between GATA2 and Notch signaling in cancer. In this study, we used in silico prediction to identify Notch3 as a target gene of GATA2, and this binding relationship was confirmed in vitro. GATA2 specifically binds to promoter region of Notch3 and enhances its transcriptional activity to promote tumor metastasis, knockdown of GATA2 significantly downregulated the expression of Notch3 and abrogated the sDLL1-mediated upregulation of NICD3 in cancer cells. Therefore, the interaction between GATA family and Notch signaling mediates distinctive biological processes, our study provided a framework to explore the transcriptional activity of Notch3 regulated by GATA2 in cancer metastasis. In conclusion, we revealed the characteristic gene expression patterns of liver metastatic

Hs766T-L3, and suggested that the activation of Notch3 signaling regulated by the TF GATA2 played a critical role in metastasis of Hs766T-L3.

Note: Supplementary information is available on the Molecules and Cells website (www.molcells.org).

AUTHOR CONTRIBUTIONS

CONFLICT OF INTEREST

ORCID
Heng Lin   https://orcid.org/0000-0003-4979-9602
Peng Hu   https://orcid.org/0000-0002-8366-0308
Hongyu Zhang   https://orcid.org/0000-0003-1522-9994
Yong Deng   https://orcid.org/0000-0001-6168-4854
Zhiqing Yang   https://orcid.org/0000-0002-3060-9904
Leida Zhang   https://orcid.org/0000-0002-7302-9184

REFERENCES
Ahmed, S., Maratha, A., Butt, A.Q., Shevlin, E., and Miggin, S.M. (2013). TRIF-mediated TLR3 and TLR4 signaling is negatively regulated by ADAM15. J. Immunol. *190*, 2217-2228.

Alvarado, A.G., Thiagarajan, P.S., Mulkearns-Hubert, E.E., Silver, D.J., Hale, J.S., Alban, T.J., Turaga, S.M., Jarrar, A., Reizes, O., Longworth, M.S., et al. (2017). Glioblastoma cancer stem cells evade innate immune suppression of self-renewal through reduced TLR4 expression. Cell Stem Cell *20*, 450-461.e4.

Angkasekwinai, P. and Dong, C. (2021). IL-9-producing T cells: potential players in allergy and cancer. Nat. Rev. Immunol. *21*, 37-48.

Cappello, P., Curcio, C., Mandili, G., Roux, C., Bulfamante, S., and Novelli, F. (2018). Next generation immunotherapy for pancreatic cancer: DNA vaccination is seeking new combo partners. Cancers (Basel) *10*, 51.

Clark, E.A., Golub, T.R., Lander, E.S., and Hynes, R.O. (2000). Genomic analysis of metastasis reveals an essential role for RhoC. Nature *406*, 532-535.

Cogli, L., Progida, C., Thomas, C.L., Spencer-Dene, B., Donno, C., Schiavo, G., and Bucci, C. (2013). Charcot-Marie-Tooth type 2B disease-causing RAB7A mutant proteins show altered interaction with the neuronal intermediate filament peripherin. Acta Neuropathol. *125*, 257-272.

de Pooter, R.F., Schmitt, T.M., de la Pompa, J.L., Fujiwara, Y., Orkin, S.H., and Zuniga-Pflucker, J.C. (2006). Notch signaling requires GATA-2 to inhibit myelopoiesis from embryonic stem cells and primary hemopoietic progenitors. J. Immunol. *176*, 5267-5275.

Deng, C.X. (2002). Roles of BRCA1 in centrosome duplication. Oncogene *21*, 6222-6227.

Di Genua, C., Valletta, S., Buono, M., Stoilova, B., Sweeney, C., Rodriguez-Meira, A., Grover, A., Drissen, R., Meng, Y., Beveridge, R., et al. (2020). C/EBPalpha and GATA-2 mutations induce bilineage acute erythroid leukemia through transformation of a neomorphic neutrophil-erythroid progenitor. Cancer Cell *37*, 690-704.e8.

Duan, Q., Li, H., Gao, C., Zhao, H., Wu, S., Wu, H., Wang, C., Shen, Q., and

Yin, T. (2019). High glucose promotes pancreatic cancer cells to escape from immune surveillance via AMPK-Bmi1-GATA2-MICA/B pathway. J. Exp. Clin. Cancer Res. *38*, 192.

Ducreux, M., Cuhna, A.S., Caramella, C., Hollebecque, A., Burtin, P., Goere, D., Seufferlein, T., Haustermans, K., Van Laethem, J.L., Conroy, T., et al. (2015). Cancer of the pancreas: ESMO Clinical Practice Guidelines for diagnosis, treatment and follow-up. Ann. Oncol. *26 Suppl 5*, v56-v68.

Feng, Q., Wu, X., Li, F., Ning, B., Lu, X., Zhang, Y., Pan, Y., and Guan, W. (2017). miR-27b inhibits gastric cancer metastasis by targeting NR2F2. Protein Cell *8*, 114-122.

Fidler, I.J. and Kripke, M.L. (1977). Metastasis results from preexisting variant cells within a malignant tumor. Science *197*, 893-895.

Garcia, A. and Kandel, J.J. (2012). Notch: a key regulator of tumor angiogenesis and metastasis. Histol. Histopathol. *27*, 151-156.

Hahn, C.N., Chong, C.E., Carmichael, C.L., Wilkins, E.J., Brautigan, P.J., Li, X.C., Babic, M., Lin, M., Carmagnac, A., Lee, Y.K., et al. (2011). Heritable GATA2 mutations associated with familial myelodysplastic syndrome and acute myeloid leukemia. Nat. Genet. *43*, 1012-1017.

Hawkins, S.M., Loomans, H.A., Wan, Y.W., Ghosh-Choudhury, T., Coffey, D., Xiao, W., Liu, Z., Sangi-Haghpeykar, H., and Anderson, M.L. (2013). Expression and functional pathway analysis of nuclear receptor NR2F2 in ovarian cancer. J. Clin. Endocrinol. Metab. *98*, E1152-E1162.

Hennessy, E.J., Parker, A.E., and O'Neill, L.A. (2010). Targeting Toll-like receptors: emerging therapeutics? Nat. Rev. Drug Discov. *9*, 293-307.

Hou, Y., Li, X., Li, Q., Xu, J., Yang, H., Xue, M., Niu, G., Zhuo, S., Mu, K., Wu, G., et al. (2018). STAT1 facilitates oestrogen receptor alpha transcription and stimulates breast cancer cell proliferation. J. Cell. Mol. Med. *22*, 6077-6086.

Inder, S., O'Rourke, S., McDermott, N., Manecksha, R., Finn, S., Lynch, T., and Marignol, L. (2017). The Notch-3 receptor: a molecular switch to tumorigenesis? Cancer Treat. Rev. *60*, 69-76.

Jones, S.A. and Jenkins, B.J. (2018). Recent insights into targeting the IL-6 cytokine family in inflammatory diseases and cancer. Nat. Rev. Immunol. *18*, 773-789.

Kang, Y., Siegel, P.M., Shu, W., Drobnjak, M., Kakonen, S.M., Cordon-Cardo, C., Guise, T.A., and Massague, J. (2003). A multigenic program mediating breast cancer metastasis to bone. Cancer Cell *3*, 537-549.

Karreth, F.A. and Pandolfi, P.P. (2013). ceRNA cross-talk in cancer: when ce-bling rivalries go awry. Cancer Discov. *3*, 1113-1121.

Leatherwood, J. (1998). Emerging mechanisms of eukaryotic DNA replication initiation. Curr. Opin. Cell Biol. *10*, 742-748.

Li, D., Xie, K., Wolff, R., and Abbruzzese, J.L. (2004). Pancreatic cancer. Lancet *363*, 1049-1057.

Liang, M., Ma, Q., Ding, N., Luo, F., Bai, Y., Kang, F., Gong, X., Dong, R., Dai, J., Dai, Q., et al. (2019). IL-11 is essential in promoting osteolysis in breast cancer bone metastasis via RANKL-independent activation of osteoclastogenesis. Cell Death Dis. *10*, 353.

Lin, J., Hou, K.K., Piwnica-Worms, H., and Shaw, A.S. (2009). The polarity protein Par1b/EMK/MARK2 regulates T cell receptor-induced microtubule-organizing center polarization. J. Immunol. *183*, 1215-1221.

Liu, C., Shi, J., Li, Q., Li, Z., Lou, C., Zhao, Q., Zhu, Y., Zhan, F., Lian, J., Wang, B., et al. (2019a). STAT1-mediated inhibition of FOXM1 enhances gemcitabine sensitivity in pancreatic cancer. Clin. Sci. (Lond.) *133*, 645-663.

Liu, J., Qu, L., Meng, L., and Shou, C. (2019b). Topoisomerase inhibitors promote cancer cell motility via ROS-mediated activation of JAK2-STAT1-CXCL1 pathway. J. Exp. Clin. Cancer Res. *38*, 370.

Menendez-Gonzalez, J.B., Sinnadurai, S., Gibbs, A., Thomas, L.A., Konstantinou, M., Garcia-Valverde, A., Boyer, M., Wang, Z., Boyd, A.S., Blair, A., et al. (2019). Inhibition of GATA2 restrains cell proliferation and enhances apoptosis and chemotherapy mediated apoptosis in human

GATA2 overexpressing AML cells. Sci. Rep. *9*, 12212.

Meurette, O. and Mehlen, P. (2018). Notch signaling in the tumor microenvironment. Cancer Cell *34*, 536-548.

Mohan, C.D., Rangappa, S., Preetham, H.D., Chandra Nayaka, S., Gupta, V.K., Basappa, S., Sethi, G., and Rangappa, K.S. (2020). Targeting STAT3 signaling pathway in cancer by agents derived from Mother Nature. Semin. Cancer Biol. 2020 Apr 20 [Epub]. https://doi.org/10.1016/j.semcancer.2020.03.016

Poste, G. and Fidler, I.J. (1980). The pathogenesis of cancer metastasis. Nature *283*, 139-146.

Radtke, F., MacDonald, H.R., and Tacchini-Cottier, F. (2013). Regulation of innate and adaptive immunity by Notch. Nat. Rev. Immunol. *13*, 427-437.

Ramaswamy, S., Ross, K.N., Lander, E.S., and Golub, T.R. (2003). A molecular signature of metastasis in primary solid tumors. Nat. Genet. *33*, 49-54.

Robert-Moreno, A., Espinosa, L., de la Pompa, J.L., and Bigas, A. (2005). RBPjkappa-dependent Notch function regulates Gata2 and is essential for the formation of intra-embryonic hematopoietic cells. Development *132*, 1117-1126.

Rosas-Salvans, M., Scrofani, J., Modol, A., and Vernos, I. (2019). DnaJB6 is a RanGTP-regulated protein required for microtubule organization during mitosis. J. Cell Sci. *132*, jcs227033.

Rothenberg, E.V. and Scripture-Adams, D.D. (2008). Competition and collaboration: GATA-3, PU.1, and Notch signaling in early T-cell fate determination. Semin. Immunol. *20*, 236-246.

Roy-Luzarraga, M. and Hodivala-Dilke, K. (2016). Molecular pathways: endothelial cell FAK-a target for cancer treatment. Clin. Cancer Res. *22*, 3718-3724.

Ryan, N., Anderson, K., Volpedo, G., Hamza, O., Varikuti, S., Satoskar, A.R., and Oghumu, S. (2020). STAT1 inhibits T-cell exhaustion and myeloid derived suppressor cell accumulation to promote antitumor immune responses in head and neck squamous cell carcinoma. Int. J. Cancer *146*, 1717-1729.

Screpanti, I., Bellavia, D., Campese, A.F., Frati, L., and Gulino, A. (2003). Notch, a unifying target in T-cell acute lymphoblastic leukemia? Trends Mol. Med. *9*, 30-35.

Siegel, R.L., Miller, K.D., and Jemal, A. (2017). Cancer statistics, 2017. CA Cancer J. Clin. *67*, 7-30.

Siegel, R.L., Miller, K.D., and Jemal, A. (2019). Cancer statistics, 2019. CA Cancer J. Clin. *69*, 7-34.

Singel, S.M., Cornelius, C., Batten, K., Fasciani, G., Wright, W.E., Lum, L., and Shay, J.W. (2013). A targeted RNAi screen of the breast cancer genome identifies KIF14 and TLN1 as genes that modulate docetaxel chemosensitivity in triple-negative breast cancer. Clin. Cancer Res. *19*, 2061-2070.

Song, S.H., Jeon, M.S., Nam, J.W., Kang, J.K., Lee, Y.J., Kang, J.Y., Kim, H.P., Han, S.W., Kang, G.H., and Kim, T.Y. (2018). Aberrant GATA2 epigenetic dysregulation induces a GATA2/GATA6 switch in human gastric cancer. Oncogene *37*, 993-1004.

Spinner, M.A., Sanchez, L.A., Hsu, A.P., Shaw, P.A., Zerbe, C.S., Calvo, K.R., Arthur, D.C., Gu, W., Gould, C.M., Brewer, C.C., et al. (2014). GATA2 deficiency: a protean disorder of hematopoiesis, lymphatics, and immunity. Blood *123*, 809-821.

Strebhardt, K. (2010). Multifaceted polo-like kinases: drug targets and antitargets for cancer therapy. Nat. Rev. Drug Discov. *9*, 643-660.

Sukhov, A., Adamopoulos, I.E., and Maverakis, E. (2016). Interactions of the immune system with skin and bone tissue in psoriatic arthritis: a comprehensive review. Clin. Rev. Allergy Immunol. *51*, 87-99.

Takebe, N., Nguyen, D., and Yang, S.X. (2014). Targeting notch signaling pathway in cancer: clinical development advances and challenges. Pharmacol. Ther. *141*, 140-149.

Tang, X., Shi, L., Xie, N., Liu, Z., Qian, M., Meng, F., Xu, Q., Zhou, M., Cao, X., Zhu, W.G., et al. (2017). SIRT7 antagonizes TGF-beta signaling and inhibits breast cancer metastasis. Nat. Commun. *8*, 318.

van 't Veer, L.J., Dai, H., van de Vijver, M.J., He, Y.D., Hart, A.A., Mao, M., Peterse, H.L., van der Kooy, K., Marton, M.J., Witteveen, A.T., et al. (2002). Gene expression profiling predicts clinical outcome of breast cancer. Nature *415*, 530-536.

Vidal, S.J., Rodriguez-Bravo, V., Quinn, S.A., Rodriguez-Barrueco, R., Lujambio, A., Williams, E., Sun, X., de la Iglesia-Vicente, J., Lee, A., Readhead, B., et al. (2015). A targetable GATA2-IGF2 axis confers aggressiveness in lethal prostate cancer. Cancer Cell *27*, 223-239.

Walden, M., Tian, L., Ross, R.L., Sykora, U.M., Byrne, D.P., Hesketh, E.L., Masandi, S.K., Cassel, J., George, R., Ault, J.R., et al. (2019). Metabolic control of BRISC-SHMT2 assembly regulates immune signalling. Nature *570*, 194-199.

Wang, F., Xia, X., Yang, C., Shen, J., Mai, J., Kim, H.C., Kirui, D., Kang, Y., Fleming, J.B., Koay, E.J., et al. (2018). SMAD4 gene mutation renders pancreatic cancer resistance to radiotherapy through promotion of autophagy. Clin. Cancer Res. *24*, 3176-3185.

Zhou, X.Z. and Lu, K.P. (2016). The isomerase PIN1 controls numerous cancer-driving pathways and is a unique drug target. Nat. Rev. Cancer *16*, 463-478.